Cancer Management and Research

Dovepress

open access to scientific and medical research

Open Access Full Text Article

ORIGINAL RESEARCH

Blocking circ_0013912 Suppressed Cell Growth, Migration and Invasion of Pancreatic Ductal Adenocarcinoma Cells in vitro and in vivo Partially Through Sponging miR-7-5p

This article was published in the following Dove Press journal:
Cancer Management and Research

Weisheng Guo[1]
Lin Zhao[1]
Guangya Wei[1]
Peng Liu[1]
Yu Zhang[1]
Liran Fu[2]

[1]Department of Hepatobiliary Surgery, Henan Province Hospital of Traditional Chinese Medicine, The Second Affiliated Hospital of Henan University of Traditional Chinese Medicine, Zhengzhou, Henan 450002, People's Republic of China; [2]Department of Traditional Chinese Medicine, People's Hospital of Zhengzhou, Zhengzhou 450000, Henan, People's Republic of China

Background: Circular RNAs have been emerging as biomarkers in diagnosis and prognosis of pancreatic ductal adenocarcinoma (PDAC). The hsa_circ_0013912 (circ_0013912) has been retrieved to be upregulated in PDAC. Here, we further investigated its role in PDAC cells, as well as its mechanism via serving as competing endogenous RNA (ceRNA) for miRNA (miR)-7-5p, which is abundant in pancreas and suppresses the development of PDAC.

Materials and Methods: The clinical human tissues were harvested from Gene Expression Omnibus (GEO) database and PDAC patients, and expression of circ_0013912 and miR-7-5p was detected by real-time quantitative PCR. The interaction between both was confirmed by dual-luciferase reporter assay, RNA immunoprecipitation and biotin-miRNA pull-down assay. Functional experiments were performed using Cell Counting Kit-8 assay, colony formation assay, fluorescence-activated cell separation method, caspase 3 activity assay kit, Western blotting, transwell assays, and xenograft tumor model.

Results: circ_0013912 was upregulated in PDAC tumors and cells; besides, circ_0013912 upregulation was associated with TNM stage and lymph node metastasis. Silencing circ_0013912 inhibited cell viability, colony formation ability, cell cycle entrance, migration and invasion, but facilitated apoptosis rate and caspase 3 activity in PANC-1 and AsPC-1 cells, accompanied with decreased c-myc, cyclin D1 and vimentin, and increased E-cadherin. Furthermore, miR-7-5p was a target of circ_0013912. Blocking miR-7-5p could promote cell growth, migration and invasion of PANC-1 and AsPC-1 cells with circ_0013912 silencing or not. Tumor growth was also restrained by circ_0013912 downregulation.

Conclusion: Circ_0013912 knockdown could suppress cell growth and metastasis of PDAC cells via sponging miR-7-5p.

Keywords: circ_0013912, miR-7-5p, PDAC

Introduction

Pancreatic ductal adenocarcinoma (PDAC) is the most prevalent type of pancreatic cancer (about 90%), and its mortality closely parallels incidence.[1] The incidence of PDAC has been ascending, and PDAC is going to be the second leading risk of cancer-associated mortality with a rate of approximate 95%.[2] Furthermore, the prognosis of PDAC is rather disillusionary with a less than 10% of 5-year survival.[3] The hallmarks of PDAC include non-typical symptoms, tardive

Correspondence: Liran Fu
Department of Traditional Chinese Medicine, People's Hospital of Zhengzhou, No. 33 Huanghe Road, Zhengzhou, Henan 450000, People's Republic of China
Tel +86-15837117112
Email w2qcxz@163.com

submit your manuscript | www.dovepress.com
DovePress
http://doi.org/10.2147/CMAR.S255808

symptoms, and lack of effective biomarkers, making it delayed diagnosis, incurable, tumor metastasis and recurrence. Nowadays, the potentially curative treatment of PDAC remains radical surgery.[4,5] Whereas data show that no more than 20% PDAC patients are capable to receive resection.[6] Therefore, it is imperative and paramount to discover effective and stable biomarkers for the prognosis of PDAC.

Circular RNAs (circRNAs) are a class of endogenous RNAs with a covalently closed continuous loop. CircRNAs are abundant in the cytoplasm of eukaryotic cells, and are resistant to endonuclease digestion.[7] These intrinsic features confer complicated functions on circRNAs in human diseases including cancer.[8] Moreover, circRNAs have been reported to be promising diagnostic and prognostic markers in many cancers including pancreatic cancer,[9,10] and exhibit tissue/developmental-stage-specific expression. The circRNAs expression profile has been revealed in PDAC tissue[11,12] and plasma.[13] The hsa_circ_0013912 (circ_0013912) was declared to be one of the top 20 upregulated circRNAs in PDAC tissues than paracancerous tissues according to Gene Expression Omnibus (GEO) database.[12] However, the role of circ_0013912 in the initiation and development of PDAC remains to be elucidated.

The circRNA-related competing endogenous RNA (ceRNA) network has been a popular molecular mechanism of the pathogenesis and treatment of PDAC.[14,15] However, the circ_0013912-microRNAs (miRNAs) interaction is left to be identified. MiRNAs are another type of endogenous noncoding RNAs with 22–24 nucleotides in a single linear structure. MiRNA (miR)-7-5p is abundant in the pancreas, and plays an important role in pancreatic development.[16] In cancer, miR-7-5p participates in multiple cancer progressions, including PDAC, through functioning as a tumor suppressor.[17,18] Furthermore, miR-7-5p has been proposed as a potential biomarker for the differentiation between PDAC and other diseases.[19,20] Therefore, we aimed to explore the expression and role of circ_0013912 and miR-7-5p in PDAC cell progression, as well as the relationship between both.

Materials and Methods

Clinical Human Tissue Samples

A set of 54 patients with PDAC without any antineoplastic treatment were recruited before undergoing pancreaticoduodenectomy surgery at Henan Province Hospital of Traditional Chinese Medicine, The Second Affiliated Hospital of Henan University of Traditional Chinese Medicine. The clinicopathological factors of this cohort of PDAC patients were summarized in Table 1. The approval of the Ethics Committee of Henan Province Hospital of Traditional Chinese Medicine, The Second Affiliated Hospital of Henan University of Traditional Chinese Medicine, and written informed consents of all patients were obtained prior to clinical tissue sample collection. Afterwards, the paired PDAC tumor tissues and paracancerous tissues were harvested during surgery. The PDAC patients were classified according to TNM stage (I–II and III) or lymph node (LN) metastasis (LN-positive or LN-negative).

Cells and Cell Transfection

Two human PDAC cell lines PANC-1 (cat. 87,092,802) and AsPC-1 (cat. 96,020,930) were from the European Collection of Authenticated Cell Cultures (Public Health England) and cultured in RPMI-1640 medium (Gibco, Grand Island, NY, USA); one normal human pancreatic duct epithelial cell line HPDE-6/E6E7 was from the Cell Collection Committee of the Chinese Academy of Sciences (Shanghai, China), and cultivated in DMEM medium (Gibco). All cells were incubated in medium plus 10% fetal bovine serum (FBS; Gibco) in cell incubator at 37°C

Table 1 Association of Circ_0013912 Expression with Clinicopathological Factors in PDAC Patients

Clinicopathological Features	Number of Cases	Circ_0013912 Expression		P value
		Low n (%)	High n (%)	
Age				
>60 years	24	10(37.0%)	14(51.9%)	0.273
≤60 years	30	17(63.0%)	13(48.1%)	
Gender				
Male	25	12(44.4%)	13(48.1%)	0.785
Female	29	15(55.6%)	14(51.9%)	
Tumor size (cm)				
>4	33	18(66.7%)	15(55.6%)	0.402
≤4	21	9(33.3%)	12(44.4%)	
TNM stage				
I+II	32	21(77.8%)	11(40.7%)	0.006
III	22	6(22.2%)	16(59.3%)	
Lymph node metastasis				
Negative	26	17(63.0%)	9(33.3%)	0.029
Positive	28	10(37.0%)	18(66.7%)	

with 5% CO_2. For cell transfection, 50 nM of siRNAs target circ_0013912 (si-circ-1 and si-circ-2), miR-7-5p mimic and inhibitor were incubated with Lipofectamine 2000 (Invitrogen, Carlsbad, CA, USA) in line with manufacture's protocol, as well as the corresponding negative controls.

Real-Time Quantitative PCR (RT-qPCR)

The tissues and cells were isolated in Trizol reagent (Invitrogen), and total RNA samples were obtained. For RNase R treatment, total RNA in cells was incubated with 3 U/μg of RNase R (Sigma-Aldrich, St Louis, MO, USA) for 20 min at 37°C, followed by purification using RNA clean kit (Axygen, Hangzhou, China) according to the instruction. The RNA expression was evaluated by SYBR Select Master Mix kit (Thermo Fisher Scientific, Waltham, MA, USA) with special RT-qPCR primer sets on ABI 7900 (Applied Biosystems, Carlsbad, CA, USA). The sequence of primer sets was circ_0013912: 5′-AGATTGTGCGA ACCATGCTC-3′ and 5′-CATCATCTGGAATGGGCTCA -3′, miR-7-5p: 5′-CGGCGGTGGAAGACTAGTGATTT-3′ and 5′-GTGCAGGGTCCGAGGT-3′, GAPDH, 5′-GACAG TCAGCCGCATCTTCT-3′ and 5′-GCGCCCAATACGAC CAAATC-3′, and U6: 5′-CTCGCTTCGGCAGCACA-3′ and 5′-CTCGCTTCGGCAGCACA-3′. The cycle threshold (Ct) value of each gene was used to examine relative expression of circ_0013912 (GAPDH as internal control) and miR-7-5p (U6 as internal control) using the $2^{-\Delta\Delta Ct}$ method. For subcellular distribution of circ_0013912, Cytoplasmic & Nuclear RNA Purification Kit (BioVision, San Francisco, USA) was utilized to obtain total RNA in cytoplasmic fraction and nuclear fraction, followed with RT-qPCR analysis as above mentioned.

Cell Viability Assay and Colony Formation Assay

After transfection, cell viability of PANC-1 and AsPC-1 cells was measured by Cell Counting Kit (CCK)-8 (Dojindo, Rockville, MD, USA), and was reflected by the optical density (OD) values at 450 nm after incubation with CCK-8 reagent at 24, 48 and 72 h. Transfected PANC-1 and AsPC-1 cells at 48 h was re-seeded in 6-well plate at density of 500 cells per well for another 14 days. Then, the cell colonies were fixed with 4% paraformaldehyde and stained with 0.5% crystal violet. Then, the image of plates was captured, and stained colonies were quantified using Image J software (National Institutes of Health).

Fluorescence-Activated Cell Separation (FACS) Methods

The transfected PANC-1 and AsPC-1 cells at 48 h were harvested and stained with Annexin V-Fluorescein Isothiocyanate (FITC) and propidium iodide (PI) according to the working manual of Annexin V-FITC/PI Apoptosis Detection Kit (Beyotime, Shanghai, China) for apoptosis rate assay; for cell cycle analysis, cells were harvested and fixed with 75% ice-cold ethanol at 4°C overnight. The DNA content in cells was stained with 50 mg/mL of PI (Sigma-Aldrich) plus 1 mg/mL RNase A and 0.2% Triton-X100 in the dark for 30 min. Then, the stained cells were analyzed by accuri C6 flow cytometer (BD Biosciences, San Jose, CA, USA), and the percentages of apoptotic cells and cells in G0/G1, S and G2/M phases were shown on CellQuest™ software 5.1 (BD Biosciences).

Caspase 3 Activity Assay

The transfected PANC-1 and AsPC-1 cells at 48 h were harvested to determine caspase 3 activity using Caspase 3 Activity Assay Kit (Beyotime) as per the manufacturer's protocol. In brief, the cell suspension was added with 100 μL of lysis buffer for 15 min on ice prior to centrifugation (15,000 g for 20 min). The supernatant was added with 10μL of Ac-DEVD-pNA (2mM) for 1 h at 37°C. OD value at 405 nm was measured on a microplate reader.

Western Blotting

Total protein in transfected PANC-1 and AsPC-1 cells at 48 h was lysed in ice-cold RIPA reagent (Invitrogen), and protein samples were split in aliquots. Equally, 25 μg proteins were subjected to the standard Western blotting procedures. The special primary antibodies were from Proteintech (Wuhan, China) including c-myc (cat. 10,828-1-AP, 1:5000), cyclin D1 (cat. 26,939-1-AP, 1:2000), E-cadherin (cat. 20,874-1-AP, 1:25,000), vimentin (cat. 10,366-1-AP, 1:10,000), and β-actin (cat. 20,536-1-AP, 1:5000). The gray density of protein bands was detected using Image J software (National Institutes of Health) to reflect relative protein expression with normalization to β-actin.

Transwell Assays

Forty-eight hours post-transfection, PANC-1 and AsPC-1 cells (1×10^5) were re-suspended in 200 μL of serum-free RPMI-1640 containing mitomycin C (1 μg/mL; Sigma-Aldrich)

(to prevent cell proliferation), and the ability of migration and invasion was measured by Transwell Permeable Supports (8.0 μm; Costar, New York, NY, USA). For migration assay, cell suspension was loaded in the top of chambers in 24-well plate, and 400 μL of RPMI-1640 plus 10% FBS was pipetted in the below of chambers. The plate was then incubated in cell incubator for another 48 h. The transferred cells adhering the lower surface were fixed with 4% paraformaldehyde and stained with 0.5% crystal violet, and then the number of migratory cells was counted from three fields of each insert under light microscopy (100×). For invasion assay, the chambers were pre-coated with Basement Membrane Matrix (BD Biosciences).

Dual-Luciferase Reporter Assay

The wild type (wt) of circ_0013912 containing GUCUUCCA was mutated into CAGAAGGA using the Quickchange XL Site-Directed Mutagenesis Kit (Agilent Stratagene, Cedar Creek, Texas, USA) according to the manufacturer's protocol. Then, wt-circ_0013912 and its mutant (mut-circ_0013912) were separately amplified in pGL4 vectors (Promega, Madison, WI, USA). PANC-1 and AsPC-1 cells in 24-well plate were co-transfected with 0.5 μg vectors and 20 nM miR-7-5p mimic or miR-NC mimic for another 48 h. The dual-luciferase activities of Firefly and Renilla (internal control) were measured on Dual-Luciferase Reporter Assay System (Promega).

RNA Immunoprecipitation (RIP) and Biotin-miRNA Pull-Down Assay

For RIP, cell lysates of PANC-1 and AsPC-1 cells were collected by RIP lysis buffer in EZ-magna RIP kit (Millipore, Billerica, MA, USA). Then, cell extracts were incubated with magnetic beads pre-conjugated with Ago2 antibody or IgG antibody for overnight at 4°C. After Proteinase K incubation, the beads were washed to obtain RIPs. For pull-down assay, miR-7-5p mimic and miR-NC mimic were biotinylated using T7 RNA polymerase (Promega) and biotinylated RNA-tagged mixtures (Roche, Basel, Switzerland). PANC-1 and AsPC-1 cells were transfected with biotinylated miR-7-5p mimic and miR-NC mimic (bio-miR-7-5p and bio-miR-NC) for 48 h, and cell lysates were collected by RIP lysis buffer for incubation of Steptavidin MagnetSphere Paramagnetic beads (Promega) for 6 h at 4°C. The RNA expression in RIP portion and biotin-miRNA pull-down portion was further detected by RT-qPCR.

Xenograft Tumor Model

A number of 12 female BALB/c nude mice (5-week-old) were purchased from the Laboratory Animal Center of Shanghai Academy of Science. These mice were randomly divided into two groups with inoculation of AsPC-1 cells transfected with shRNA target circ_0013912 (sh-circ; n=6) or sh-NC (n=6). The shRNAs were synthesized from Sangon Biotech (Shanghai, China), and this animal study was performed following the Guide for the Care and Use of Laboratory Animals of the National Institutes of Health. Briefly, 1×10^7 cells were subcutaneously injected into the left armpits of mice, and tumor sizes including the length (L) and the perpendicular width (W) were measured using a caliper every week for 5 times after inoculation. On the last week, xenograft tumors were separated and weighted after the mice were sacrificed. The tumor volume was calculated using the equation: $0.5\times LW^2$. This xenograft study was approved by the Ethics Committee of Henan Province Hospital of Traditional Chinese Medicine, The Second Affiliated Hospital of Henan University of Traditional Chinese Medicine.

Statistical Analysis

The quantitative data were shown as the mean±standard deviation. Unpaired Student's *t*-test was employed to compare the difference between two groups, and one-way analysis of variance followed with Turkey's post hoc test was for comparisons in multiple groups on GraphPad Prism version 5.00 (GraphPad Software, San Diego, CA, USA). Two-tailed Pearson's correlation (*r*) analysis was used to determine the association between the expression of circ_0013912 and miR-7-5p. P value less than 0.05 was significant difference.

Results

circ_0013912 Was Upregulated in Human PDAC Tumor Tissues

To confirm the deregulated circRNAs in PDAC, the raw microarray data of circRNAs in GEO database was analyzed. According to GSE79634 dataset and GSE69362 dataset, the heatmap showed the most 10 upregulated circRNAs in PDAC tissues comparing to paracancerous tissues, and circ_0013912 was shown to be upregulated in

both datasets (Figure 1A and B). With researching circPrimer software, we found that circ_0013912 was derived from exon 6 and exon 7 of RNA polymerase III subunit C (POLR3C) gene via back-splicing, with a mature sequence length of 198 nucleotides (Figure 1C). Thus, we further identify circ_0013912 expression in a set of PDAC patients using RT-qPCR. The results indicated that circ_0013912 expression level was significantly higher (1.67-fold, $P<0.05$) in PDAC tissues than adjacent normal tissues (Figure 1D). Besides, 43 out of 54 of PDAC tissues displayed increased expression of circ_0013912 (Figure 1E); level of circ_0013912 was higher in TNM III stage (Figure 1F), and LN-positive tumors (Figure 1G). Moreover, there was a significant correlation of circ_0013912 high level with advanced TNM stage and LN metastasis (Table 1). Collectively, circ_0013912 was upregulated in PDAC tumor tissues, and was associated with TNM stage and LN metastasis.

circ_0013912 Was Upregulated in Human PDAC Cells

The expression model of circ_0013912 was clarified in PDAC cells in vitro. RT-qPCR data depicted an elevation of circ_0013912 expression in PANC-1 and AsPC-1 cells compared to HPDE-6/E6E7 cells (Figure 2A). Moreover, circ_0013912 expression was little descended by RNase R treatment in PANC-1 and AsPC-1 cells; whereas, GAPDH mRNA expression was greatly decreased in response to RNase R (Figure 2B and C). The subcellular localization of circ_0013912 was further investigated, and RT-qPCR data showed circ_0013912 was mainly distributed in the cytoplasmic fraction of PANC-1 and AsPC-1 cells, which was analogous to GAPDH, and opposite to U6 (Figure 2D and E). Thereby, special siRNAs target the splice junction of circ_0013912 were synthesized to knockdown circ_0013912 expression (Figure 2F), and RT-qPCR analysis confirmed a relatively better knockdown efficiency of si-circ-1 than si-circ-2 in PANC-1 and AsPC-1 cells

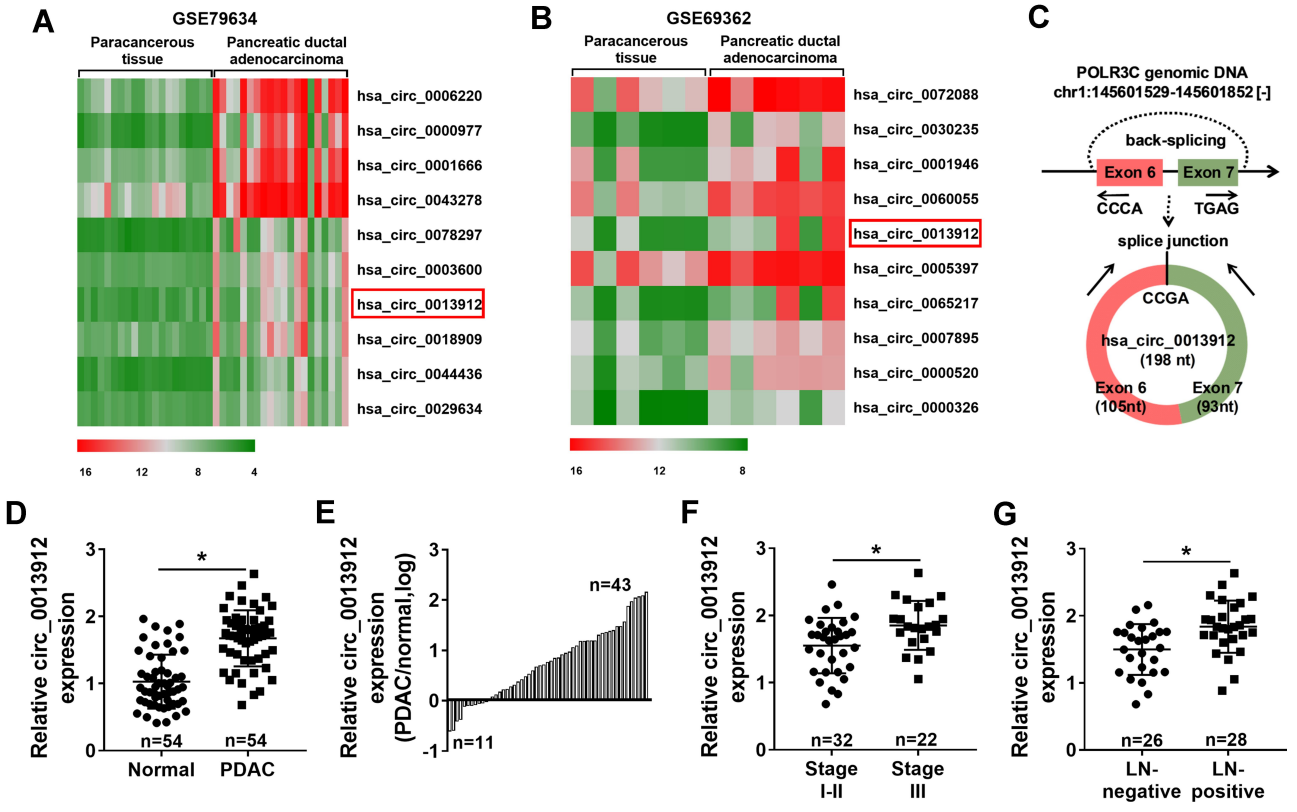

Figure 1 Expression of hsa_circ_0013912 (circ_0013912) was upregulated in pancreatic ductal adenocarcinoma (PDAC) tumors. (**A, B**) The heatmap showed the top 10 upregulated circRNAs in PDAC tumor tissues and paracancerous tissues according to (**A**) GSE79634 dataset and (**B**) GSE69362 dataset. (**C**) The schematic diagram showed circ_0013912 was back-spliced from POLR3C gene. (**D, E**) RT-qPCR detected circ_0013912 expression level in 54 paired PDAC tissues (PDAC) and adjacent normal tissues (Normal). (**F, G**) RT-qPCR detected circ_0013912 expression in (**F**) TNM stage I–II (n=32) and stage III (n=22), and (**G**) lymph node (LN)-positive tumors (n=28) and LN-negative tumors (n=26). *$P<0.05$.

(Figure 2G). These results indicated that circ_0013912 was stably and highly expressed in cytoplasm of PDAC cells.

Blocking circ_0013912 Suppressed Cell Growth, Migration and Invasion in PDAC Cells in vitro

Taken Figures 1 and 2 together, we hypothesized that circ_0013912 probably functioned a pivotal role in malignant progression of PDAC. Thus, we studied the effect of circ_0013912 knockdown on cell growth, migration and invasion in PDAC cells in vitro. CCK-8 revealed that cell viability of PANC-1 and AsPC-1 cells were inhibited due to si-circ-1 transfection (Figure 3A), and colony formation assay showed a decrease of colony number in si-circ-1-administrated PANC-1 and AsPC-1 cells (Figure 3B). Furthermore, FACS method determined that circ_00013912 knockdown via si-circ-1 transfection reduced S phase cells, but increased G0/G1 phase cells in PANC-1 and AsPC-1 cells (Figure 3C), as accompanied with apoptotic cells promotion (Figure 3D). Commercial assay kit evaluated that caspase 3 activity was also enhanced by si-circ-1 treatment, paralleled with si-NC treatment (Figure 3E). Expression of markers of cell proliferation was measured by Western blotting, and the data depicted that c-myc and cyclin D1 protein levels were declined in PANC-1 and AsPC-1 cells with si-circ-1 insults (Figure 3F and G). Transwell assays examined cell migration and invasion of PANC-1 and AsPC-1 cells, and si-circ-1 transfection resulted in a lowered number of migratory cells and invasive cells than si-NC group (Figure 4A and B), along with promoted E-cadherin and depressed vimentin (Figure 4C and D). These results demonstrated that blocking circ_0013912 could suppress PDAC cell growth, migration and invasion in vitro, hinting a tumor-suppressive role of circ_0013912 knockdown in PDAC.

circ_0013912 Was a Sponge for miR-7-5p in PDAC Cells

We used three types of miRNA target prediction software including circinteractome, starbase and circbank to predict the potential miRNAs targeting circ_0013912. There were two common miRNAs among these three bioinformatics algorithms, namely miR-877-5p and miR-7-5p (Figure 5A). The regulatory sensitivity of circ_0013912 on miRNAs was monitored, and RT-qPCR data manifested that only miR-7-5p was distinctively upregulated in si-circ-1-transfected PANC-1 and AsPC-1 cells (Figure 5B). Subsequently, the

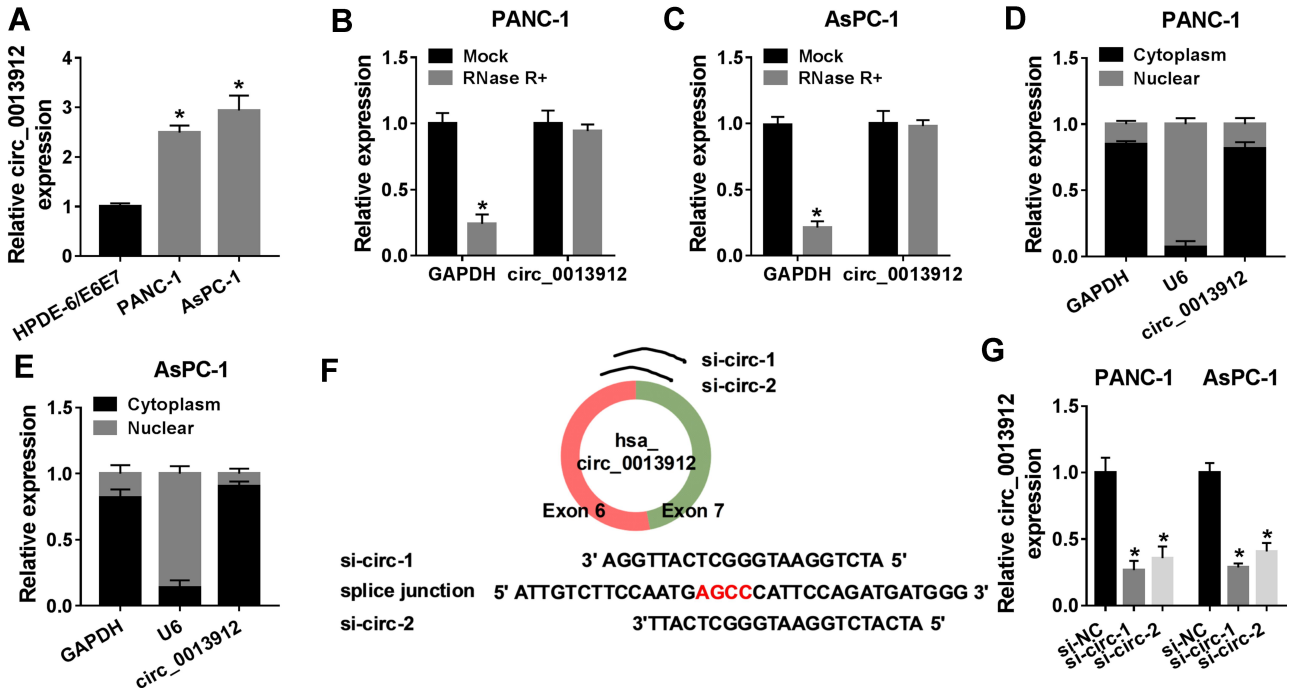

Figure 2 The expression of circ_0013912 in human PDAC cells in vitro. (**A**) RT-qPCR assessed circ_0013912 expression level in PANC-1 and AsPC-1 cells, compared to normal human pancreatic duct epithelial cells HPDE-6/E6E7. (**B, C**) RT-qPCR assessed RNA expression of circ_0013912 and glyceraldehyde-phosphate dehydrogenase (GAPDH) in PANC-1 and AsPC-1 cells after RNase R treatment or not. (**D, E**) RT-qPCR assessed RNA expression of circ_0013912, GAPDH and U6 in cytoplasmic fraction and nuclear fraction of PANC-1 and AsPC-1 cells. (**F**) The schematic diagram showed siRNAs target splice junction of circ_0013912 (si-circ-1 and si-circ-2). (**G**) RT-qPCR assessed circ_0013912 expression level in PANC-1 and AsPC-1 cells transfected si-circ-1, si-circ-2 or the negative control si-NC. *P<0.05.

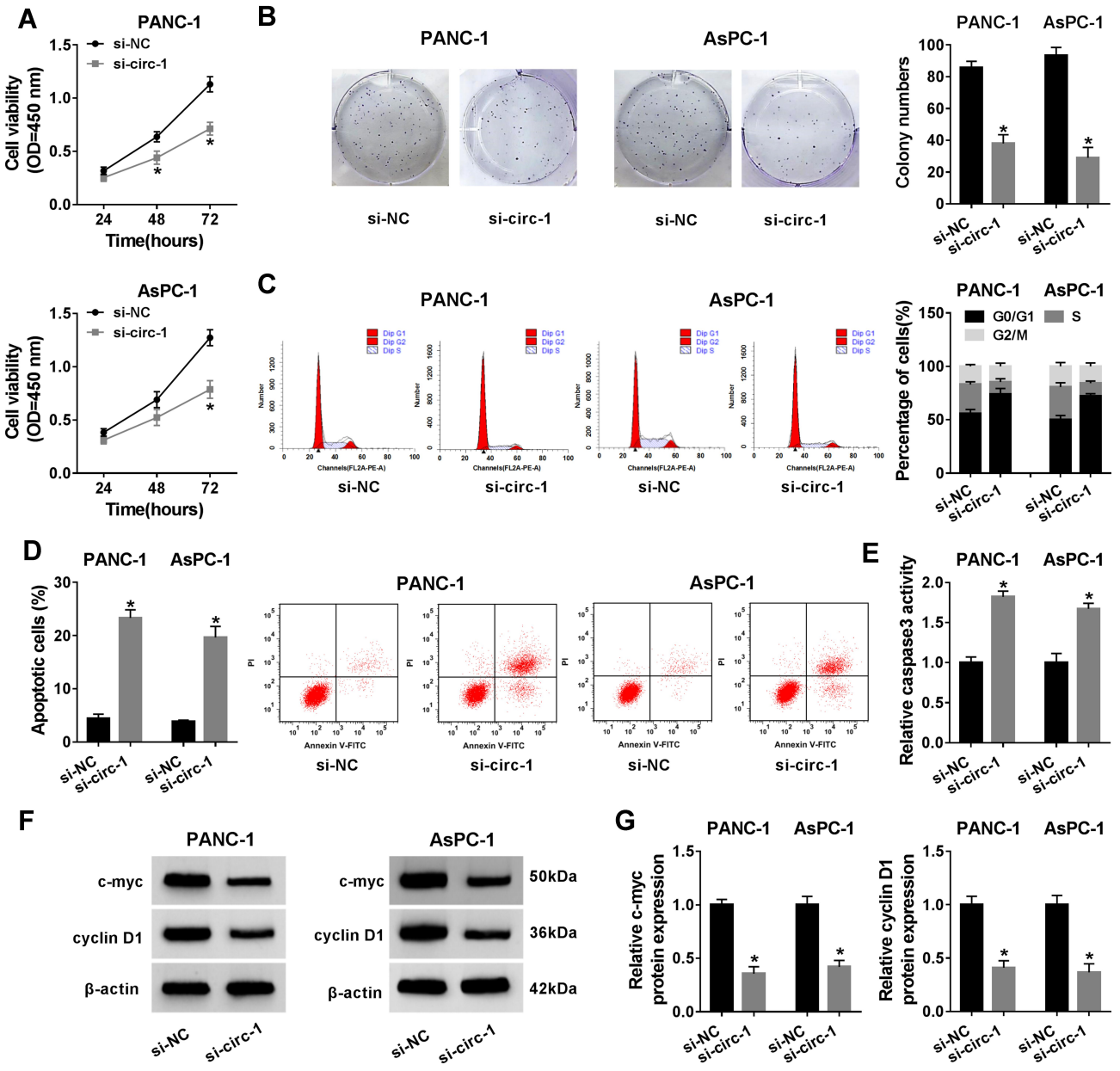

Figure 3 The role of circ_0013912 knockdown in cell growth and apoptosis in PDAC cells in vitro. (**A**–**G**) PANC-1 and AsPC-1 cells were transfected with si-circ-1 or si-NC for 48 h. (**A**) CCK-8 assay evaluated cell viability. **Notes:** OD, optical density. (**B**) Colony numbers were determined by colony formation assay. (**C, D**) Fluorescence-activated cell separation (FACS) method determined the percentages of (**C**) cells in G0/G1, S and G2/M phases, and (**D**) apoptotic cells. (**E**) Caspase 3 assay kit estimated caspase 3 activity. (**F, G**) Western blotting examined protein expression of c-myc and cyclin D1, compared to β-actin. **P*<0.05.

potential circ_0013912-miR-7-5p interaction was further testified according to the putative complementary binding sites (Figure 5C). Dual-luciferase reporter assay detected that luciferase activity of wt-circ_0013912 vectors was markedly declined in the presence of miR-7-5p mimic in both PANC-1 and AsPC-1 cells (Figure 5D); meanwhile, mut-circ_0013912 vectors showed no altered luciferase activity whenever transfection with miR-7-5p mimic or the control. In PANC-1 and AsPC-1 cells, RIP assay suggested a simultaneous enrichment of circ_0013912 and miR-7-5p in Ago2-mediated RIP portion (Figure 5E); in addition, cic_0013912 was dramatically enriched in bio-miR-7-5p-mediated RNA pull-down portion as well (Figure 5F). These outcomes prompted a direct relationship between circ_0013912 and miR-7-5p in PDAC cells. Besides, the expression of miR-7-5p in PDAC was investigated. As shown in Figure 5G and H, miR-7-5p level was downregulated in PDAC cell lines and tumor tissues (Figure 5G and H); there were 81.5% (44/54) PDAC patients with low expression of miR-7-5p (Figure 5I). Pearson correlation

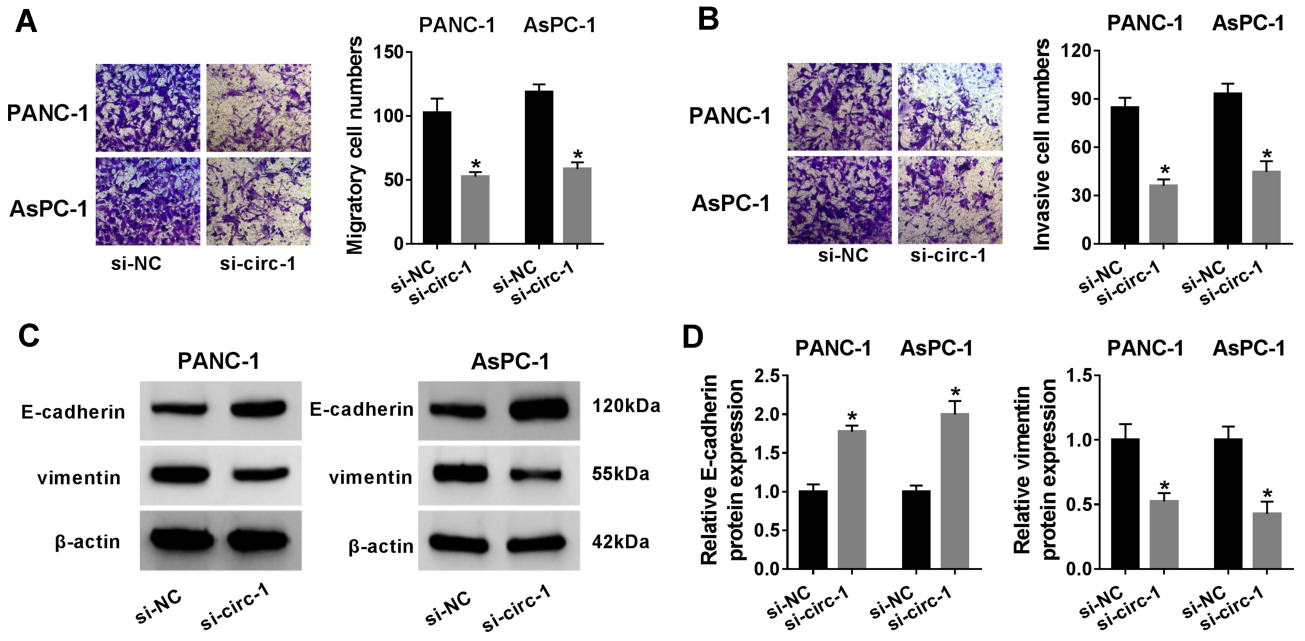

Figure 4 The role of circ_0013912 knockdown in cell migration and invasion in PDAC cells in vitro. (**A–D**) PANC-1 and AsPC-1 cells were transfected with si-circ-1 or si-NC for 48 h. (**A, B**) Transwell assay showed numbers of migratory cells and invasive cells (100×). (**C, D**) Western blotting examined protein expression of E-cadherin and vimentin, compared to β-actin. *P<0.05.

analysis identified an inverse correlation between circ_0013912 and miR-7-5p expression in PDAC tissues (Figure 5J). These results indicated that circ_0013912 might serve as a molecular sponge for miR-7-5p in PDAC cells.

Deficiency of miR-7-5p Promoted Cell Growth, Migration and Invasion of PDAC Cells in vitro, and Partially Reversed the Tumor-Suppressive Role of circ_0013912 Knockdown

The effect of miR-7-5p deficiency was further figured out in PDAC cells with or without circ_0013912 knockdown. PANC-1 and AsPC-1 cells were transfected with si-circ-1 alone, miR-7-5p inhibitor (anti-miR-7-5p) to silence its expression (Figure 6A). The functional experiments were performed in PANC-1 and AsPC-1 cells, and cell viability was facilitated by miR-7-5p downregulation (Figure 6B); moreover, blocking miR-7-5p could concurrently enhance colony number (Figure 6C), S phase cells (Figure 6D), numbers of migratory cells and invasive cells (Figure 6G and H), and expression of c-myc, cyclin D1 and vimentin (Figure 6I and J) in PANC-1 and AsPC-1 cells. Meanwhile, anti-miR-7-5p transfection led to inhibition on G0/GI phase cells (Figure 6D), apoptotic cells (Figure 6E), caspase 3 activity (Figure 6F), and E-cadherin expression (Figure 6I and J). Collectively, miR-7-5p downregulation exerted the opposite effects of circ_0013912 knockdown on cell growth, migration and invasion of PDAC cells in vitro (Figure 6B–J). Notably, co-transfection of si-circ-1 and anti-miR-7-5p could partially reverse the suppressive role of circ_0013912 deficiency in cell growth, migration and invasion of PANC-1 and AsPC-1 cells, as well as the promoting role of miR-7-5p deletion (Figure 6B–J). All in all, we considered that a circ_0013912/miR-7-5p axis in the progression of PDAC in vitro.

Blocking circ_0013912 Inhibited Cell Growth and Metastasis of PDAC Cells in vivo

The animal study was further performed to elucidate the role of circ_0013912 in vivo. AsPC-1 cells transfected sh-circ or sh-NC were transplanted into node mice (n=6), and the tumors were harvested on 5 week after inoculation. As shown in Figure 7A and B, sh-circ led to restrained tumor volume and less tumor weight. The expression of circ_0013912 was lower and miR-7-5p was higher in xenograft tumor tissues (Figure 7C and D); furthermore, c-myc, cyclin D1 and vimentin protein expression was also downregulated, accompanied with E-cadherin promotion (Figure 7E). These data demonstrated that blocking circ_0013912 could suppress cell growth, migration and invasion of PDAC cells in vivo.

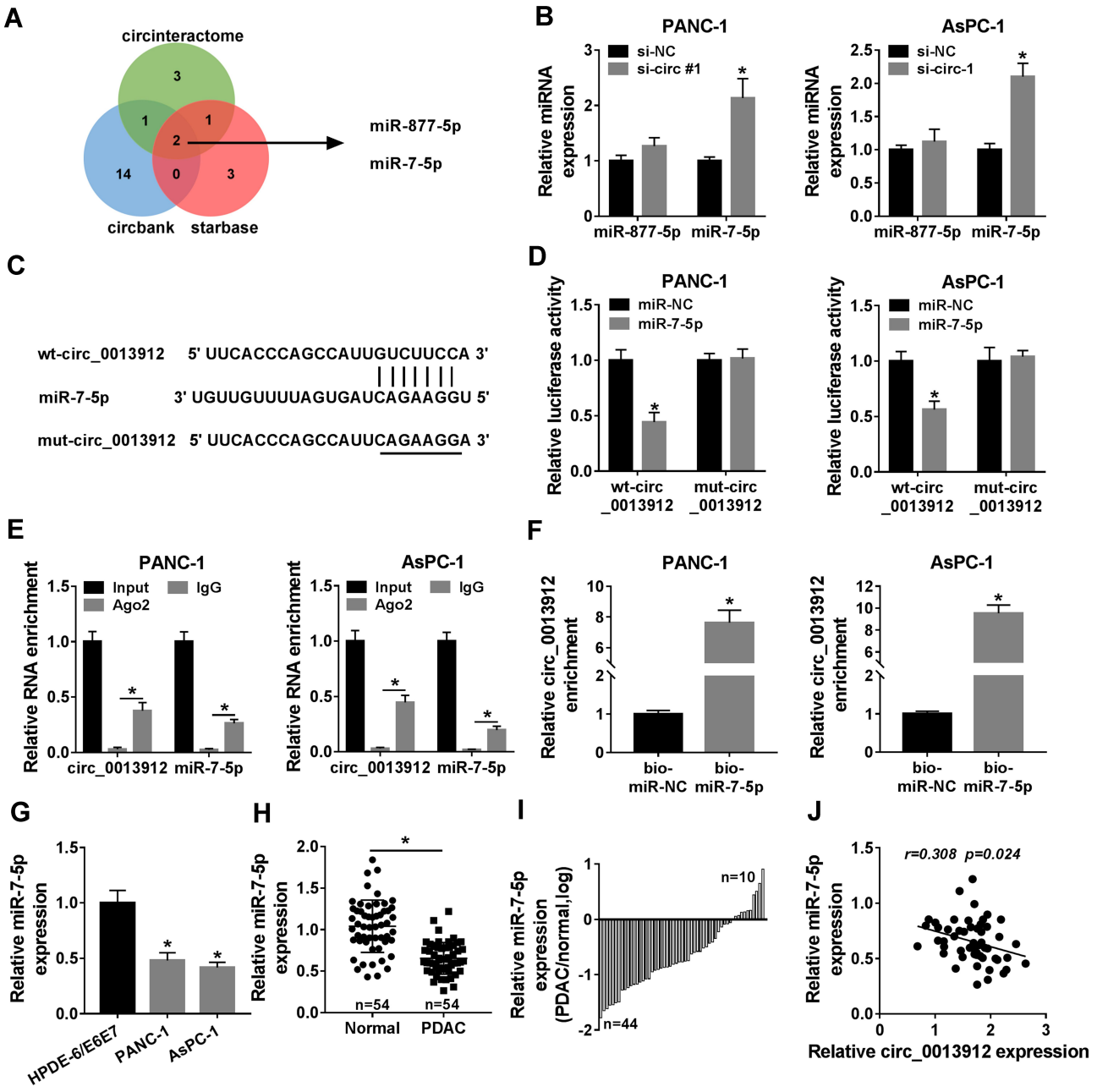

Figure 5 Circ_0013912 was a sponge for miRNA (miR)-7-5p in PDAC cells. (**A**) Venn Diagram showed the common miRNAs that potentially targeting circ_0013912 according to circinteractome, starbase and circbank data. (**B**) RT-qPCR detected expression levels of miR-877-5p and miR-7-5p in PANC-1 and AsPC-1 cells transfected with si-circ-1 or si-NC for 48 h. (**C**) The sequences of wild type (wt) of circ_0013912 (wt-circ_0013912) and its mutant (mut-circ_0013912). (**D**) Dual-luciferase reporter assay measured luciferase activity of PANC-1 and AsPC-1 cells co-transfected with wt/mut-circ_0013912 and miR-7-5p/miR-NC mimic (miR-7-5p/miR-NC) for 48 h. (**E**) RNA immunoprecipitation (RIP) assay measured the enrichment of circ_0013912 and miR-7-5p in Ago2 portion and IgG portion of PANC-1 and AsPC-1 cells. (**F**) Biotin-miRNA pull-down assay verified circ_0013912 enrichment in PANC-1 and AsPC-1 cells transfected with biotinylated miR-7-5p or miR-NC (bio-miR-7-5p or bio-miR-NC) for 48 h. (**G–I**) RT-qPCR examined miR-7-5p expression in (**G**) HPDE-6/E6E7, PANC-1 and AsPC-1 cells, and (**H, I**) 54 paired PDAC samples and Normal samples. (**J**) Pearson correlation analysis identified a correlation between circ_0013912 and miR-7-5p expression in PDAC tumor tissues (n=54). *P<0.05.

Discussion

Due to delayed presentation, tumor metastasis and recurrence, PDAC remained to be a devastating disease. CircRNAs had been emerging but promising biomarkers for early diagnosis and prognosis, and therapeutic target for the treatment of PDAC,[21] because of their imperative and diversiform functions in tumorigenesis and tumor progression. Several types of circRNAs had been identified to be prognostic biomarkers for overall survival of PDAC patients, such as circ_0001649, circ_0007534 and

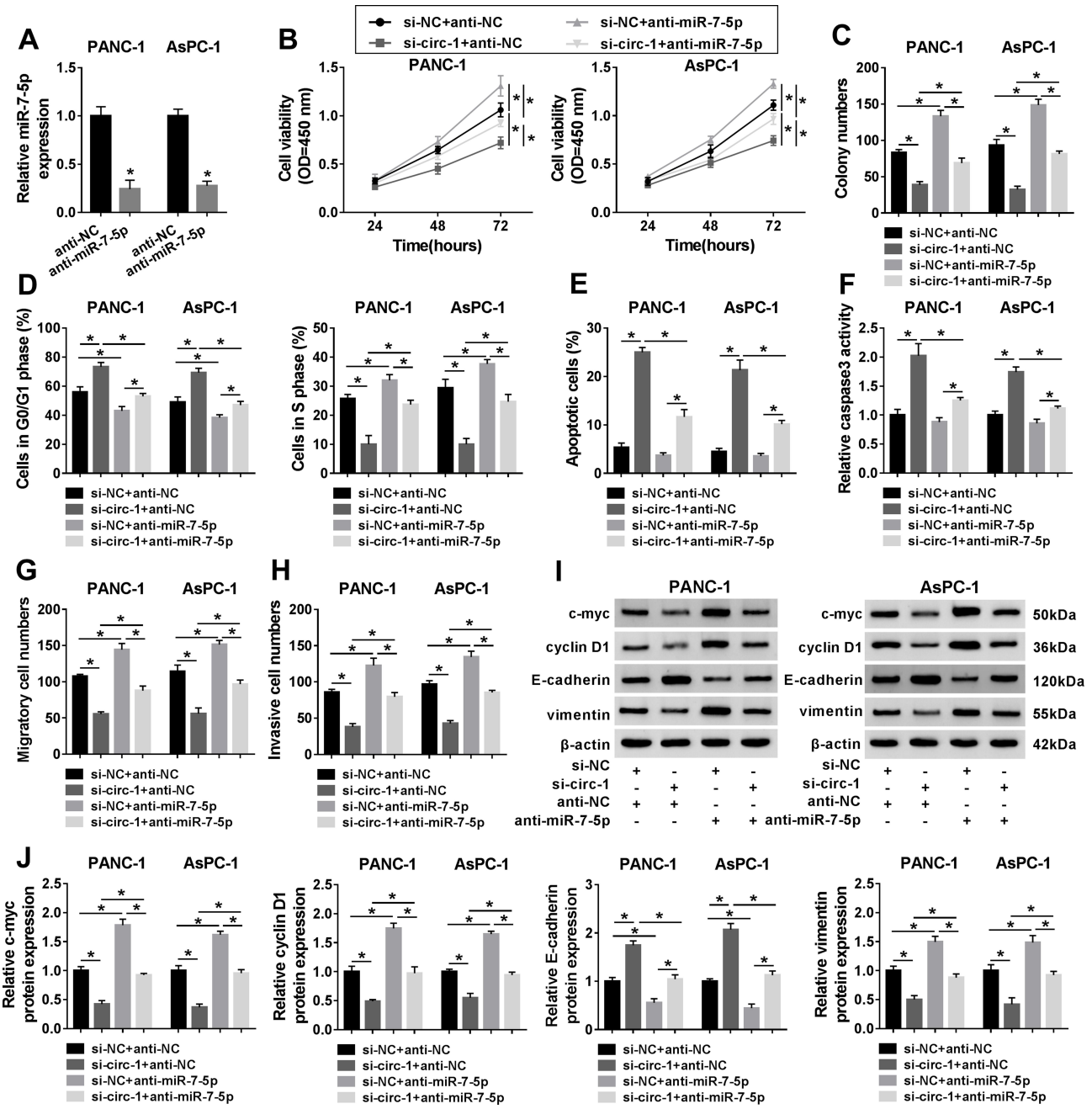

Figure 6 The effect of miR-7-5p and circ_0013912 in PDAC cells in vitro. (**A**) RT-qPCR detected miR-7-5p expression in PANC-1 and AsPC-1 cells transfected with miR-7-5p inhibitor (anti-miR-7-5p) or the negative control anti-NC. (**B–J**) PANC-1 and AsPC-1 cells were co-transfected with si-NC and anti-NC, si-circ-1 and anti-NC, si-NC and anti-miR-7-5p, si-circ-1 and anti-miR-7-5p. (**B**) CCK-8 assay evaluated cell viability. (**C**) Colony numbers were determined by colony formation assay. (**D, E**) FACS method determined the percentages of (**D**) cells in G0/G1 and S phases, and (**E**) apoptotic cells. (**F**) Caspase 3 assay kit estimated caspase 3 activity. (**G, H**) Transwell assay showed numbers of migratory cells and invasive cells (100×). (**I, J**) Western blotting examined protein expression of c-myc, cyclin D1, E-cadherin, and vimentin, compared to β-actin. **P*<0.05.

circ_0030235.[22–24] Moreover, these circRNAs were also correlated with clinicopathological parameters of PDAC patients, including tumor stage and LN invasion. Here, we discovered that circ_0013912 was upregulated in most (79.6%) of PDAC tissues, advanced TNM stage and LN metastasis. Taken the anti-growth, anti-migration and anti-invasion role of circ_0013912 knockdown in PDAC cells in vitro and in vivo into consideration, we proposed circ_0013912 as a novel potential biomarker of PDAC diagnosis. By the way, it was reported that circulating circRNAs could also be reliable non-invasive biomarkers for monitor and diagnosis of PDAC.[25] Therefore, it could

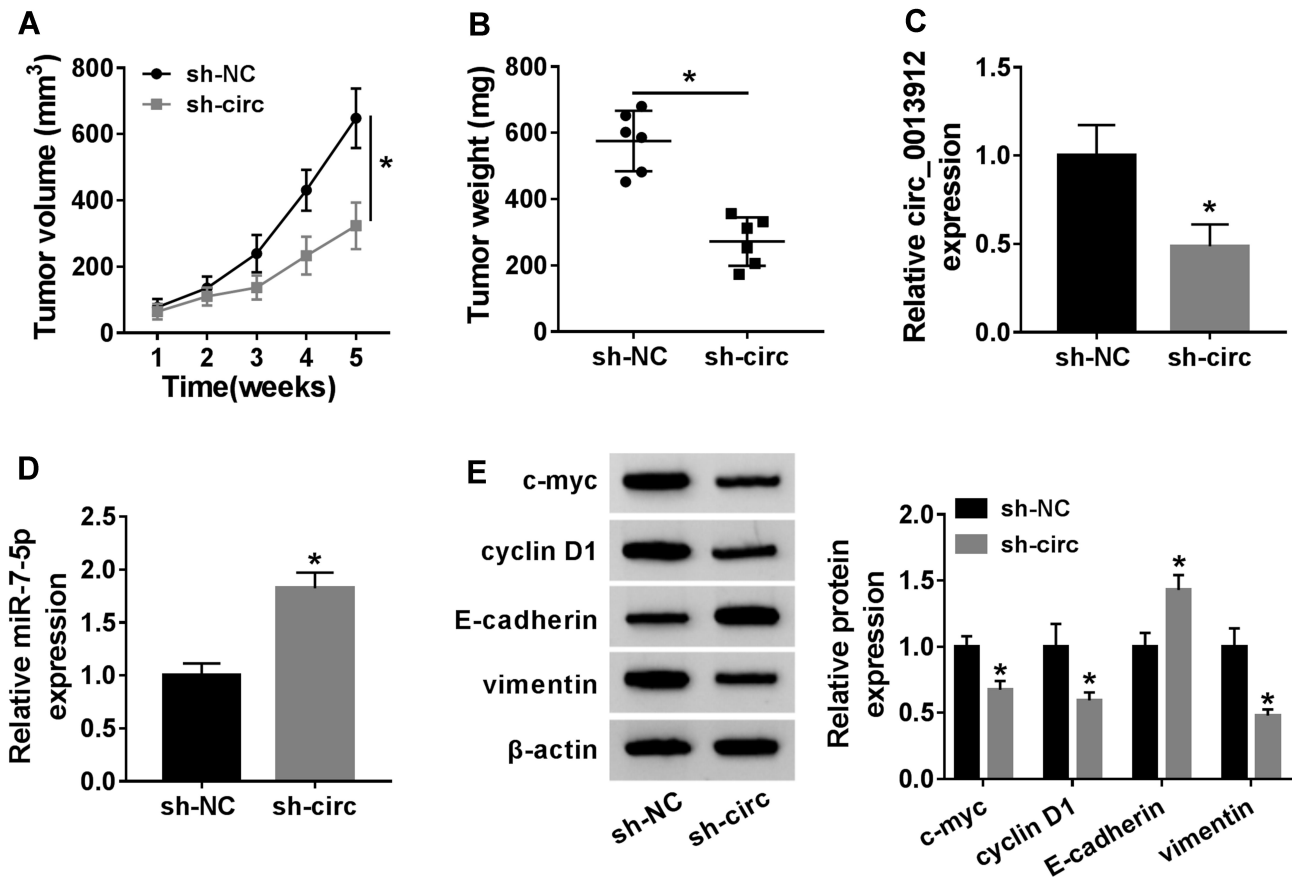

Figure 7 Blocking circ_0013912 inhibited cell growth and metastasis of PDAC cells in vivo. Xenograft tumors (n=6) were generated to test tumor growth. (**A, B**) The volume and weight of tumors were measured. (**C, D**) RT-qPCR detected circ_0013912 and miR-7-5p expression levels in tumor tissues from mice. (**E**) Western blotting evaluated protein levels of c-myc, cyclin D1, E-cadherin and vimentin in tumor tissues from mice. *P<0.05.

also be intriguing to identify the expression of circ_00013912 in plasma of PDAC patients in the further.

With researching GSE69362 and GSE79634 datasets, we obtained the top 10 upregulated circRNAs in PDAC tumor tissues, and found that circ_0013912 was the common circRNA in the two lists. The upregulation of circ_0013912 was consistent with previous analysis based on GEO database.[12] Circ_0013912 was derived from exon 6 and 7 of POLR3C gene, and also known as hsa_circPOLR3C_008 according to circbank. The expression of circ_0013912 was resistant to RNase R degradation, and the subcellular distribution of circ_0013912 was overwhelmingly in cytoplasm. All these information suggested a pivotal role of circ_0013912 in PDAC cell progression. Thus, the siRNAs targeting the splice junction of circ_0013912 were designed and testified. Loss-of-function experiments demonstrated that silencing of circ_0013912 could increase apoptosis rate, caspase 3 activity and E-cadherin expression in PDAC cells in vitro, but decrease cell viability, colony formation, cell cycle entrance, migration, invasion, and expression of c-myc, cyclin D1, and vimentin, which were biomarkers of cell proliferation and invasion. Furthermore, circ_0013912 knockdown could also restrained carcinogenicity of AsPC-1 cells in vivo, as accompanied with lower c-myc, cyclin D1, and vimentin, and higher E-cadherin. Aforementioned findings suggested a suppressive role of circ_0013912 knockdown in PDAC cell growth, migration and invasion in vitro and in vivo.

According to Zhang et al,[12] there was a circ_0013912-miR-577 interaction according to prediction of miRanda and RNAhybrid algorithms. Here, we sought out miR-7-5p and miR-877-5p as promising target miRNAs for circ_0013912 depending on in silico data on circinteractome, circbank and starbase. Further, we confirmed the direct relationship between circ_0013912 and miR-7-5p in PDAC cells. MR-7-5p was a tumor suppressor in PDAC. For example, overexpression of miR-7-5p was declared to inhibit proliferation, migration and invasion of PANC-1 and PaTu-8988 cells in vitro and tumor growth in vivo through targeting ILF2, MAP3K9 and SOX18.[18,26,27] Besides, cell autophagy of

SW1990 and PANC-1 cells was suppressed by miR-7-5p upregulation by targeting LKB1, ULK2, ATG4A and ATG7, thus interfering glycolysis.[28] Furthermore, miR-7-5p was involved in cancer stem cells suppression and drug resistance.[29,30] Here, we supported the downregulation of miR-7-5p in PDAC tissues and cell lines,[18,26,27] and this low expression could contribute to cell proliferation, colony formation, cell cycle entrance, migration and invasion of PANC-1 and AsPC-1 cells with circ_0013912 knockdown or not. The proliferation and invasion of AsPC-1 and BxPC-3 cells were restrained by miR-7-5p overexpression,[31] as well. Thereby, our data demonstrated a tumor-promoting role of miR-7-5p deficiency in PDAC cells. In addition, we considered that miR-7-5p was sponged by circ_0013912 to modulate PDAC cell growth, migration and invasion. Other reports determined ciRS-7/miR-7-5p axis in multiple tumor cells[32–34] including PDAC cells.[35] Taken together, we suggested a circRNAs-miR-7-5p network and circ_0013912-miRNAs network underlying PDAC tumorigenesis. However, even though previous study had expounded the important part of miR-7-5p in clinical diagnosis and prognosis in PDAC,[18] here we did not investigate the correlation among tumor stage, LN metastasis and miR-7-5p just like circ_0013912.

The interaction network analysis had constructed a miR-7-5p gene network through targeting RAF1, PIK3, IGF1R, AKT3, etc.[29] Whereas the downstream functional genes of circ_0013912-miR-7-5p axis were left to be further explored, as well as other vital cell behaviors, such as epithelial-mesenchymal transition and autophagy.[26,28] Additionally, the relevant signaling pathways should also be detected, such as JAK/STAT3, AMPK-mTOR, MAPK and NF-kB pathways.[18,27,28] Recently, a series of imidazo[2,1-b][1,3,4]thiadiazole derivatives had been synthesized and identified as new anticancer agents of PDAC;[36–38] thus it is also imperative to further detect the detail molecular mechanism of the antiproliferative activity of these derivatives, such as analyzing circ_0013912 and miR-7-5p expression.

In conclusion, this study showed that circ_0013912 was upregulated in PDAC tumor tissues and cells, and was an unfavorable biomarker for PDAC diagnosis. Knockdown of circ_0013912 inhibited cell growth, migration and invasion of PDAC cells in vitro and in vivo by sponging miR-7-5p. Therefore, we suggested circ_0013912-miR-7-5p axis as a novel promising clinical target for the diagnosis and treatment of PDAC.

Funding

There is no funding to report.

Disclosure

The authors declare that they have no financial conflicts of interest.

References

1. Siegel RL, Miller KD, Jemal A. Cancer statistics, 2019. *CA Cancer J Clin*. 2019;69(1):7–34. doi:10.3322/caac.21551
2. Rahib L, Smith BD, Aizenberg R, Rosenzweig AB, Fleshman JM, Matrisian LM. Projecting cancer incidence and deaths to 2030: the unexpected burden of thyroid, liver, and pancreas cancers in the United States. *Cancer Res*. 2014;74(11):2913–2921. doi:10.1158/0008-5472.CAN-14-0155
3. Miller KD, Siegel RL, Lin CC, et al. Cancer treatment and survivorship statistics, 2016. *CA Cancer J Clin*. 2016;66(4):271–289. doi:10.3322/caac.21349
4. Hartwig W, Werner J, Jager D, Debus J, Buchler MW. Improvement of surgical results for pancreatic cancer. *Lancet Oncol*. 2013;14(11):e476–e485. doi:10.1016/S1470-2045(13)70172-4
5. Kulkarni NM, Soloff EV, Tolat PP, et al. White paper on pancreatic ductal adenocarcinoma from society of abdominal radiology's disease-focused panel for pancreatic ductal adenocarcinoma: part I, AJCC staging system, NCCN guidelines, and borderline resectable disease. *Abdom Radiol*. 2020;45(3):716–728. doi:10.1007/s00261-019-02289-5
6. Hidalgo M, Cascinu S, Kleeff J, et al. Addressing the challenges of pancreatic cancer: future directions for improving outcomes. *Pancreatology*. 2015;15(1):8–18. doi:10.1016/j.pan.2014.10.001
7. Li JQ, Yang J, Zhou P, et al. Circular RNAs in cancer: novel insights into origins, properties, functions and implications. *Am J Cancer Res*. 2015;5(2):472–480.
8. Lee ECS, Elhassan SAM, Lim GPL, et al. The roles of circular RNAs in human development and diseases. *Biomed Pharmacother*. 2019;111:198–208. doi:10.1016/j.biopha.2018.12.052
9. Naeli P, Pourhanifeh MH, Karimzadeh MR, et al. As and gastrointestinal cancers: epigenetic regulators with a prognostic and therapeutic role. *Crit Rev Oncol Hematol*. 2020;145:102854. doi:10.1016/j.critrevonc.2019.102854
10. Jiang PC, Bu SR. Clinical value of circular RNAs and autophagy-related miRNAs in the diagnosis and treatment of pancreatic cancer. *Hepatobiliary Pancreat Dis Int*. 2019;18(6):511–516. doi:10.1016/j.hbpd.2019.09.009
11. Li HM, Hao XK, Wang MH, et al. Circular RNA expression profile of pancreatic ductal adenocarcinoma revealed by microarray. *Cell Physiol Biochem*. 2016;40(6):1334–1344. doi:10.1159/000453186
12. Zhang Q, Wang JY, Zhou SY, Yang SJ, Zhong SL. Circular RNA expression in pancreatic ductal adenocarcinoma. *Oncol Lett*. 2019;18(3):2923–2930. doi:10.3892/ol.2019.10624
13. Li QQ, Geng SS, Yuan HX, et al. Circular RNA expression profiles in extracellular vesicles from the plasma of patients with pancreatic ductal adenocarcinoma. *FEBS Open Bio*. 2019;9(12):2052–2062. doi:10.1002/2211-5463.12741
14. Zhou JZ, Hu MR, Diao HL, Wang QW, Huang Q, Ge BJ. Comprehensive analysis of differentially expressed circRNAs revealed a ceRNA network in pancreatic ductaladenocarcinoma. *Arch Med Sci*. 2019;15(4):979–991. doi:10.5114/aoms.2019.85204
15. Xiao Y. Construction of a circRNA-miRNA-mRNA network to explore the pathogenesis and treatment of pancreatic ductal adenocarcinoma. *J Cell Biochem*. 2020;121(1):394–406. doi:10.1002/jcb.29194

16. Chen WQ, Hu L, Chen GX, Deng HX. Role of microRNA-7 in digestive system malignancy. *World J Gastrointest Oncol*. 2016;8(1):121–127. doi:10.4251/wjgo.v8.i1.121
17. Li M, Pan M, You ZC, Dou J. The therapeutic potential of miR-7 in cancers. *Mini Rev Med Chem*. 2019;19(20):1707–1716. doi:10.2174/1389557519666190904141922
18. Zhu WH, Wang YZ, Zhang DF, Yu X, Leng XS. MiR-7-5p functions as a tumor suppressor by targeting SOX18 in pancreatic ductal adenocarcinoma. *Biochem Biophys Res Commun*. 2018;497(4):963–970. doi:10.1016/j.bbrc.2018.02.005
19. Akamatsu M, Makino N, Ikeda Y, et al. Specific MAPK-associated microRNAs in serum differentiate pancreatic cancer from autoimmune pancreatitis. *PLoS One*. 2016;11(7):e0158669. doi:10.1371/journal.pone.0158669
20. Li PP, Hu YB, Yi J, Li J, Yang J, Wang J. Identification of potential biomarkers to differentially diagnose solid pseudopapillary tumors and pancreatic malignancies via a gene regulatory network. *J Transl Med*. 2015;13:361. doi:10.1186/s12967-015-0718-3
21. Wang YZ, An Y, Li BQ, Lu J, Guo JC. Research progress on circularRNAs in pancreatic cancer: emerging but promising. *Cancer Biol Ther*. 2019;20(9):1163–1171. doi:10.1080/15384047.2019.1617563
22. Jiang YH, Wang T, Yan L, Qu LJ. A novel prognostic biomarker for pancreatic ductal adenocarcinoma: hsa_circ_0001649. *Gene*. 2018;675:88–93. doi:10.1016/j.gene.2018.06.099
23. Hao LG, Rong W, Bai LJ, et al. Upregulated circular RNA circ_0007534 indicates an unfavorable prognosis in pancreatic ductal adenocarcinoma and regulates cell proliferation, apoptosis, and invasion by sponging miR-625 and miR-892b. *J Cell Biochem*. 2019;120(3):3780–3789. doi:10.1002/jcb.27658
24. Xu Y, Yao Y, Gao P, Cui YF. Upregulated circular RNA circ_0030235 predicts unfavorable prognosis in pancreatic ductal adenocarcinoma and facilitates cell progression by sponging miR-1253 and miR-1294. *Biochem Biophys Res Commun*. 2019;509(1):138–142. doi:10.1016/j.bbrc.2018.12.088
25. Li ZH, Yf W, Li J, et al. Tumor-released exosomal circular RNA PDE8A promotes invasive growth via the miR-338/MACC1/MET pathway in pancreatic cancer. *Cancer Lett*. 2018;432:237–250. doi:10.1016/j.canlet.2018.04.035
26. Bi YL, Shen W, Min M, Liu Y. MicroRNA-7 functions as a tumor-suppressor gene by regulating ILF2 in pancreatic carcinoma. *Int J Mol Med*. 2017;39(4):900–906. doi:10.3892/ijmm.2017.2894
27. Xia J, Cao T, Ma C, et al. miR-7 suppresses tumor progression by directly targeting MAP3K9 in pancreatic cancer. *Mol Ther Nucleic Acids*. 2018;13:121–132. doi:10.1016/j.omtn.2018.08.012
28. Gu DN, Jiang MJ, Mei Z, et al. microRNA-7 impairs autophagy-derived pools of glucose to suppress pancreatic cancer progression. *Cancer Lett*. 2017;400:69–78. doi:10.1016/j.canlet.2017.04.020
29. Shen Y, Pu KF, Zheng KX, et al. Differentially expressed microRNAs in MIA PaCa-2 and PANC-1 pancreas ductal adenocarcinoma cell lines are involved in cancer stem cell regulation. *Int J Mol Sci*. 2019;20(18):4473. doi:10.3390/ijms20184473
30. Tian XF, Shivapurkar N, Wu Z, et al. Circulating microRNA profile predicts disease progression in patients receiving second-line treatment of lapatinib and capecitabine for metastatic pancreatic cancer. *Oncol Lett*. 2016;11(3):1645–1650. doi:10.3892/ol.2016.4101
31. Ma J, Fang BB, Zeng FP, et al. Curcumin inhibits cell growth and invasion through up-regulation of miR-7 in pancreatic cancer cells. *Toxicol Lett*. 2014;231(1):82–91. doi:10.1016/j.toxlet.2014.09.014
32. Su CY, Han Y, Zhang HT, et al. CiRS-7 targeting miR-7 modulates the progression of non-small cell lung cancer in a manner dependent on NF-kappaB signalling. *J Cell Mol Med*. 2018;22(6):3097–3107. doi:10.1111/jcmm.13587
33. Huang HR, Wei L, Qin T, Yang N, Li ZD, Xu ZY. Circular RNA ciRS-7 triggers the migration and invasion of esophageal squamous cell carcinoma via miR-7/KLF4 and NF-kappaB signals. *Cancer Biol Ther*. 2019;20(1):73–80. doi:10.1080/15384047.2018.1507254
34. Zhang JZ, Hu HY, Zhao YX, Zhao YL. CDR1as is overexpressed in laryngeal squamous cell carcinoma to promote the tumour's progression via miR-7 signals. *Cell Prolif*. 2018;51(6):e12521. doi:10.1111/cpr.12521
35. Liu L, Liu FB, Huang M, et al. Circular RNA ciRS-7 promotes the proliferation and metastasis of pancreatic cancer by regulating miR-7-mediated EGFR/STAT3 signaling pathway. *Hepatobiliary Pancreat Dis Int*. 2019;18(6):580–586. doi:10.1016/j.hbpd.2019.03.003
36. Cascioferro S, Li Petri G, Parrino B, et al. 3-(6-phenylimidazo [2,1-b][1,3,4]thiadiazol-2-yl)-1H-indole derivatives as new anticancer agents in the treatment of pancreatic ductal adenocarcinoma. *Molecules*. 2020;25(2):329. doi:10.3390/molecules25020329
37. Cascioferro S, Petri GL, Parrino B, et al. Imidazo[2,1-b][1,3,4]thiadiazoles with antiproliferative activity against primary and gemcitabine-resistant pancreatic cancer cells. *Eur J Med Chem*. 2020;189:112088. doi:10.1016/j.ejmech.2020.112088
38. Li Petri G, Cascioferro S, El Hassouni B, et al. Biological evaluation of the antiproliferative and anti-migratory activity of a series of 3-(6-phenylimidazo[2,1-b][1,3,4]thiadiazol-2-yl)-1H-indole derivatives against pancreatic cancer cells. *Anticancer Res*. 2019;39(7):3615–3620. doi:10.21873/anticanres.13509